By Andrew Long (Andrew.Long@pgs.com)

Rock Physics: From Basics to the Validation of Advanced Seismic Technology Platforms

Five short webinars that focus on several aspects of rock physics are now available on-demand at https://www.pgs.com/techbyte. These address fundamental challenges related to the use of rock physics: How can we build robust saturated rock physics models of a heterogeneous earth? How can machine learning and geologically-consistent rock physics modeling workflows reduce exploration uncertainty? How can FWI models augmented by rock-physics transformations overcome missing low frequencies? What low-frequency amplitude and phase issues in broadband seismic data are critical to rock physics estimation workflows? How can rock physics estimation workflows validate new seismic technology platforms in frontier areas with minimal-to-no well control? Throughout the five-part mini-series, emphasis is given to rock physics being the bridge that connects geophysics and geology, and that guides QI efforts. Geologically-consistent rock models can be built that are augmented by FWI models, and FWI models can be reliably transformed into robust elastic low frequency models. With these platforms, various global case studies illustrate how carefully processed multisensor broadband seismic data can therefore be used to predict accurate lithology and fluid properties—even when well control is poor.

Introduction

Most geoscientists who work with seismic data understand how subsurface contrasts in impedance between superimposed geological formations cause seismic reflectivity to vary as a function of angle for incident wavefields ('Amplitude versus Angle or Offset: AVA or AVO). AVA / AVO information is used at a variety of scales: from screening 3D seismic volumes to identify spatial contrasts in AVO classes, to 'absolute' pre-stack simultaneous inversion of quantitatively accurate elastic attributes (P-impedance and S-impedance). Rock physics is the bridge that connects the geophysical attributes to geological properties.

There are many uncertainties that confront any such integration of geophysics and geology. How seismic data was acquired, and how it was processed, clearly has a critical influence on the final migrated image quality, and the amplitude and phase fidelity of the pre-stack data. This sensitivity is reinforced by the fact that we only have three parameters to work with: the compressional (or 'P-wave') velocity, the shear wave (or 'S-wave') velocity, and the bulk density. Once we overcome the fact that seismic data are band-limited and affected by various noise and artifacts, these three 'bottleneck' parameters are equated to saturated rock models that attempt to replicate the in-situ conditions of the seismic survey. Supported by available petrophysical data derived from borehole and laboratory measurements, these efforts will hopefully translate seismic measurements into accurate predictions of reservoir properties, with their spatial distributions throughout the subsurface.

Rock Models and Elastic Bounds

Most of the published literature (e.g. Mavko et al., 2020, and Avseth et al., 2005) is dedicated to high porosity sandstones, although considerable research is going into the more challenging domains of shale and carbonate reservoirs, including the relevance of fractures and dissolution.

Any simplified rock model is based upon a knowledge of how such rocks evolve, and broadly has two key considerations: mechanical compaction during burial as the grain packing changes, and diagenetic or cementation effects that typically start to occur at burial depths of about 2 km (and an associated temperature of about 70ºC). Before deposition, sediments exist as particles suspended in water, and their acoustic properties must fall on the

(harmonic) Reuss average of mineral and fluid in the left side of Figure 1. When the sediments are first deposited on the water bottom, their porosity at deposition is determined by the geometry of the grain packing. Upon burial, various processes give the sediment strength – effective stress, compaction, and cementation – and move the sediments off the Reuss bound. At a porosity known as the 'critical porosity', the process of lithification begins, and we observe that with increasing diagenesis—mechanical and chemical compaction—the rock properties fall along steep trajectories that extend upward from the Reuss bound at critical porosity, toward the so-called mineral end point at zero porosity. The upper Voigt bound in the left side of Figure 1 is the linear average of the same moduli. The Reuss and Voigt bounds are the largest possible bounds, and in practice, we seek more restrictive bounds based on a negligible amount of specific information relevant to the local conditions. The narrowest possible range of elastic moduli without specifying anything about the geometries of the constituents are the Hashin-Shtrikman bounds.

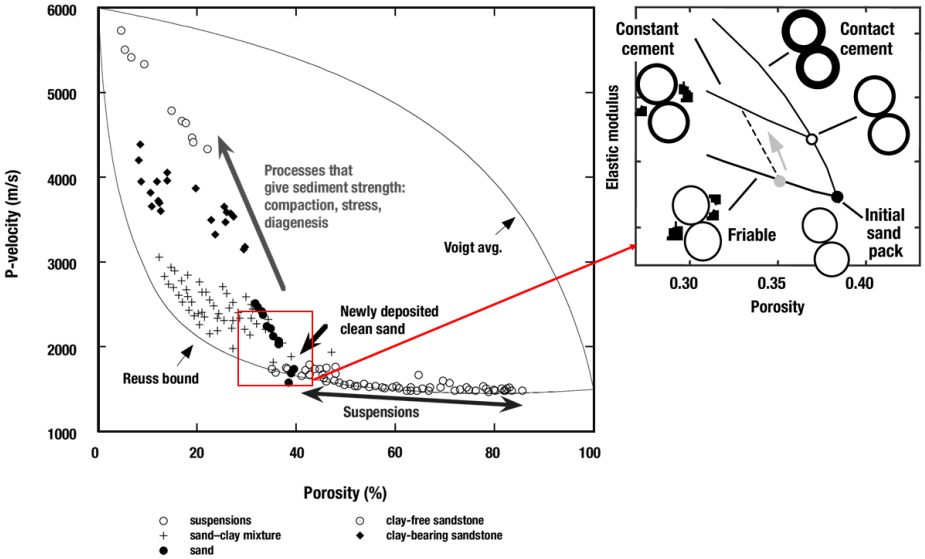

Figure 1. (left) P-wave velocity versus porosity for a variety of water-saturated sediments, compared with the Voigt-Reuss bounds; and (right) Schematic depiction of three effective-medium models for high-porosity sands in the plane of elastic modulus versus porosity, and corresponding diagenetic transformations. The elastic modulus may be compressional, bulk, or shear. Modified from Avseth et al. (2005), with permission.

Rock models are built with a common hierarchy, and with typical assumptions of isotropic, homogeneous, linear elastic media; that all minerals in the rock matrix have the same bulk and shear moduli; that the fluid-bearing rock is completely saturated; and that pore pressure is uniform throughout the pore space, all the pores are well connected, and the frequency and viscosity are low enough for any pressure differences to equilibrate during seismic wave propagation. As discussed below, the heterogeneity of the earth is accounted for by considering parameters such as the burial history, the influence of shaly minerals, temperature gradients, average grain size, and so on.

In a nutshell, and these are not the only ways of describing the observed properties of saturated rocks, two robust models can explain how a rock becomes stiffer in response to the passage of a seismic wave—and remember that is the root of everything discussed here—the response of saturated rocks to seismic waves captured in the three 'bottleneck' parameters of compressional wave velocity, shear wave velocity, and bulk density (refer also to the right side of Figure 1):

- The **constant cement model** describes the velocity-porosity behavior versus cement volume, where the cement fills the crack-like spaces near the grain contacts. It is equivalent to so-called 'poorer' sorting where we have small grains filling in the interstitial spaces between the larger grains. Cement can variously be derived from quartz, clay or carbonate.
- The **contact cement model** describes the velocity-porosity behavior versus sorting at a specific cement volume, normally corresponding to a specific depth, where cement at grain contacts acts as a type of glue, and the elastic moduli of the stiffer rock can increase quite quickly.

And there are many other published models applicable to more specific scenarios.

My first webinar titled 'The Basics of Rock Physics' considers how the analysis of trends in the cross-plot space of elastic and physical properties is used to calibrate rock physics models for specific locations. I also discuss how to account for the probabilistic variance in the distribution of elastic parameters related to specific lithologies or fluid types in a depth- and spatially-variable manner.

Every litho-fluid scenario is *different* from one location to the next. There is no universal rock physics model or AVO model. Correspondingly, the real potential of rock-physics modeling is the ability to systematically test different reservoir scenarios and how observed elastic parameters change under different conditions. Whatever the elastic moduli or parameters derived from our seismic and/or petrophysical data, by cross-plotting these elastic properties as a function of different geological scenarios in multi-dimensional space, information derived from the seismic data—such as via pre-stack AVO inversion—can be classified into geologically-meaningful categories.

Before I progress to geologically-constrained AVO analysis, Figure 2 is a quick example of how rock physics models can be used to rapidly simulate the elastic AVO response using a tool acquired and developed by PGS called rockAVO. A high-resolution 1D geological model in the left panel of Figure 2 can be perturbed for a variety of realistic scenarios using the relevant rock physics model parameters (accounting for the in-situ mechanical and chemical compaction effects, along with many other key parameters), and the elastic parameters appropriate to each depth are used to synthesize an elastic well log relevant to that 1D model. That synthetic well log is used to model the NMO-corrected pre-stack seismic gathers in the middle of Figure 2. It is very efficient to rapidly synthesize and model many such scenarios, and then reconcile the real and synthetic data to identify plausible geological models that might explain the real data. This workflow is common within the industry, but an integrated tool has been missing. The power of the real-time link of rockAVO to three-dimensional AVO feasibility analysis will shortly become obvious.

Managing Uncertainty in Quantitative Seismic Interpretation

In many exploration programs, particularly in frontier areas, there is limited well control. Even when well data is available, there is always missing or incomplete petrophysical data. The geological setting and history of reservoir rocks is often complex, and the representative seismic data may correspondingly be imperfect or ambiguous.

So we face two challenges when trying to manage uncertainty in the application of elastic attributes and AVO diagnostics to the interpretation of seismic data. First, we need a robust strategy to build useful saturated rock physics models, even when well control is poor; and second, we clearly need to account for the geological history and modern-day setting of our reservoir prospects when determining how elastic attributes and AVO diagnostics can, and cannot be applied in a reliable manner.

Where well data is available, traditional petrophysical log analysis and conditioning has historically been time-consuming and very intensive for skilled practitioners. Ruiz et al. (2021) show how the development of machine learning algorithms for the prediction of parameters such as porosity, hydrocarbon saturation, Vs, and so on, have proven to be remarkably accurate. In the case study shown, petrophysical properties are consistent within dozens of wells, and even across different geographic locations, which makes machine learning models a very promising route for accurate and efficient property estimation, as well as being extremely useful for optimizing current petrophysical and rock physics workflows. One notable benefit of the methods described is that unlike traditional empirical industry approaches, no inputs are required for mineralogy, fluid saturation, or other parameters—other than depths below mudline.

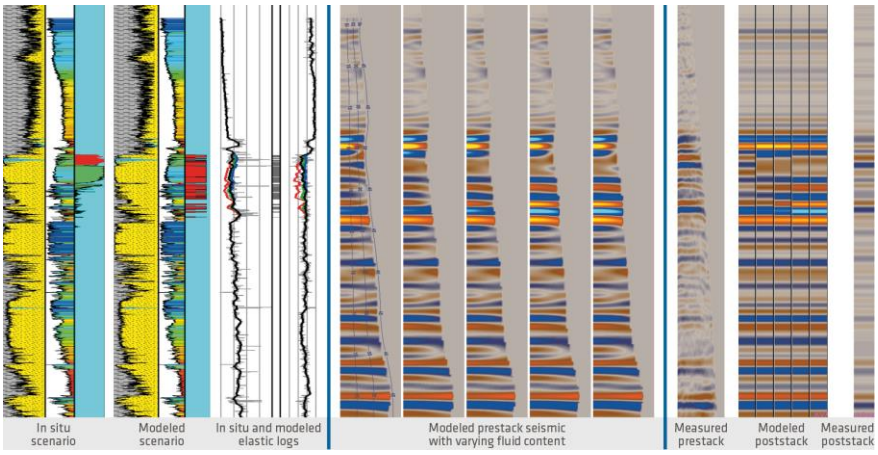

Figure 2. rockAVO example of one geological model scenario being used to model elastic logs and NMO-corrected pre-stack gathers and post-stack seismic panels, which are then compared to real in-situ data.

Three key references summarize the workflow used as the platform for building rock models in this article, and which form the introduction to my second webinar titled 'Managing Uncertainty in Rock Physics Models'. Lehocki and Avseth (2020) illustrate how to understand the physical and seismic properties of rocks by looking in detail at compaction and diagenetic modeling as a function of burial history, and then show how rock-physics modeling is sensitive to such considerations with regards to variations in the timing of the burial history, the maximum burial depths, the amount of uplift, and so on. They then show how these considerations affect the 'fluid

sensitivity' of saturated rocks when we attempt to classify them using AVO methods. Avseth and Lehocki (2021) extend this methodology to case examples from the North Sea and the Barents Sea where significant uplift exists. Key outputs are rock property and AVO feasibility maps and cubes, and an important contribution from the seismic data is the use of high-resolution velocity models to constrain the maximum burial and net erosion maps. The collaboration with PGS authors in Avseth et al. (2020) combines the workflow in the previous two papers with FWI velocity models and rapid simultaneous pre-stack seismic inversion into a workflow for real-time AVO feasibility modeling.

Table 1 is from Lehocki and Avseth (2020), and presents sequential geological processes from deposition to deep burial and uplift. The cartoons in the left column of Table 1 show the relevant stage in the burial history as a red circle corresponding to each row of geological and rock physics considerations in the table. Note how the burial history can influence the stiffness of saturated rocks, and correspondingly, the associated 'fluid sensitivity' when pursuing AVO analysis in terms of the Gradient versus the Intercept terms derived from pre-stack seismic data: The deeper the burial, the higher the degree of chemical compaction, and the smaller the separation of the distributions of AVO responses for brine versus gas saturation.

These principles are clearly demonstrated in the Barents Sea case study of Avseth et al. (2020). Combined rock physics and compaction modeling was integrated with FWI P-wave seismic velocities and basin analysis to create regional uplift and maximum burial maps for selected horizons and intervals. Geologically-consistent 3D AVO feasibility cubes were then generated from these maximum burial and net erosion maps, while also honoring key uncertainties in parameters such as rock texture, mineralogy, heterogeneity, anisotropy, temperature, and so on (refer to Figure 3). As noted already, from a rock physics point of view, the key focus is to know the maximum burial history of whatever intervals are considered—which enables one to reliably quantify the amount of diagenetic quartz cement that has been generated during burial and uplift. And as might be expected, uplift and erosion is highly dependent upon regional structural deformation.

Burial domain	Geological process	Geological parameter	Physical parameter	Rock-physics modelling
At/near surface 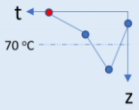	• Weathering/erosion • Sediment transport (suspension or saltation) • **Deposition** • Leaching of felspar and mica • Bioturbation	• **Mineralogic composition** • **Grain size** • **Grain shape** • **Sorting** • **Depositional porosity** • Pore structure • Lamination	• **Effective mineralogic moduli** • **Clay volume** • **Grain diameter** • **Critical porosity** • Net-to-gross	• **Elastic mixing models** (Hill's average, Hashin-Shtrikman models) • Suspension models (lower bound Hashin-Shtrikman or Reuss bounds)
Mechanical compaction domain (< 70 °C, ca. 0-2 km) 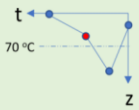	• **Grain packing** • Grain crushing/cracking • Creep/Ductile deformation • Early carbonate cementation • **Authigenic clays** • **Porosity reduction** • Opal-A → Opal-CT • Undercompaction/overpressure • Remobilization/injectites	• **Packing degree** • Grain alignment • **Clay coating (authigenic)** • Calcite cement • **Primary porosity**	• **Intergranular volume** • **Framework stability** • **Specific surface area** • **Contact area** • **Coordination number** • **Effective stress** • **Shear weakening (i.e. stress relaxations)**	• Contact theory (Hertz-Mindlin, Walton). • Modified contact theory (Bachrach and Avseth, 2008) • Friable sand model (Dvorkin and Nur, 1996) • **Combined mechanical compaction and contact theory (this paper)**
Chemical compaction domain (> 70 °C) 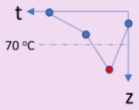	• **Stylolite dissolution** • **Quartz cementation** • Feldspar dissolution • Carbonate dissolution • Dolomitization • **Clay diagenesis**	• Stylolite distance • **Cement volume** • Cement location • Secondary porosity • **Clay volume/location** • **Burial/Temperature history**	• **Contact cement volume** • **Pore-filling cement volume** • **Temperature** • **Temperature gradient** • **Time**	• Contact cement theory (Dvorkin and Nur, 1996) • Constant cement model (Avseth et al., 2000) • Patchy cement model (Avseth et al., 2016) • **Combined chemical compaction and contact theory (this paper)**
Deeply buried, then uplifted 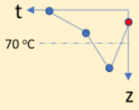	• **Tectonic uplift** • **Exhumation** • **Unloading** • Fracturing/Brittle failure	• **Continued cementation (pore-filling)** • Tensile cracks • Pore shape • **Net erosion estimate**	• **Pore-filling cement volume** • Aspect ratio • Crack density • **Effective stress** • Anisotropy	• Inclusion based models (e.g. DEM, Mori-Tanaka) • Hybrid models (e.g. Avseth et al., 2014; Bredesen et al.,2019) • **Combined mechanical/chemical compaction and contact theory (this paper)**

Table 1. Overview of geological processes acting on sands and sandstones from deposition to deep burial and uplift, and how these relate to rock-physics. The processes, together with controlling parameters and modelling approaches considered/utilized in this study, are shown in bold. It is important to note that we ignore processes like early calcite cement, feldspar dissolution, overpressure and fracturing. From Lehocki and Avseth (2021).

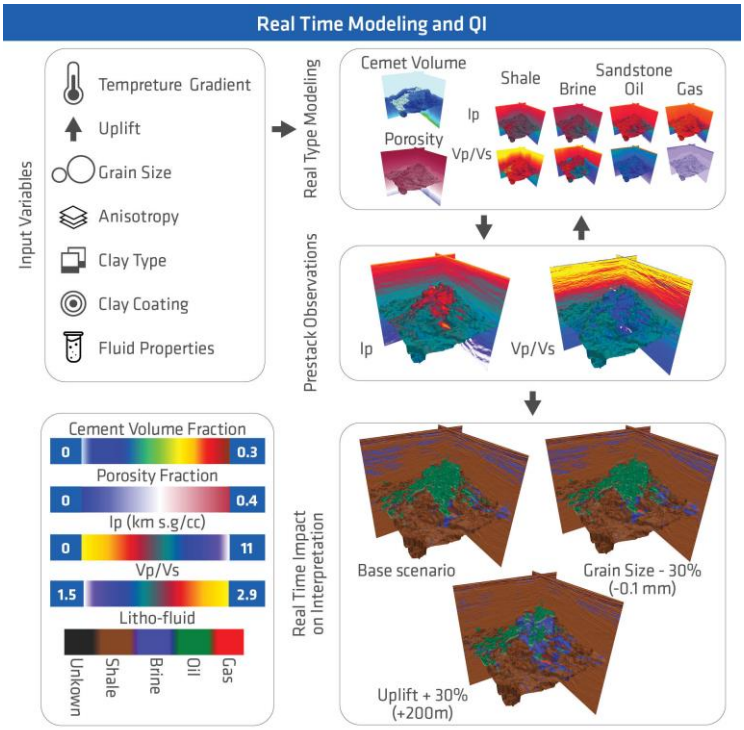

Figure 3. Sensitivity analysis for lithology and fluid derisking in 3D using real time rock physics modelling to test geological scenarios and measure the impact on the quantitative interpretation of broadband pre-stack seismic data observations. From Avseth et al. (2020b).

The resultant feasibility maps such as Figure 4 show modeled reservoir and rock properties along a target horizon in the upper row, and the lower row shows the corresponding AVO feasibility maps, for a given geological scenario. For this specific set of input parameters—one of many considered in a real study—the reservoir shows significant fluid sensitivities and strong AVO anomalies when saturated with hydrocarbons. As shown in Figure 4, there will likely be a change in the AVO class from Class 1 to 2p for a brine-saturated reservoir—the lower left panel—to Class 3 when saturated with relatively light oil or gas—the lower right hand panels. This workflow can be applied for entire 3D AVO feasibility and rock property cubes. According to the geological history-driven workflow mentioned here, geological scenarios and uncertainties in the input parameters—also listed in the upper left panel of Figure 3—can be tested on the desktop in real time, and the resulting simulated AVO and rock property cubes can be compared with real data in the impedance or reflectivity domains.

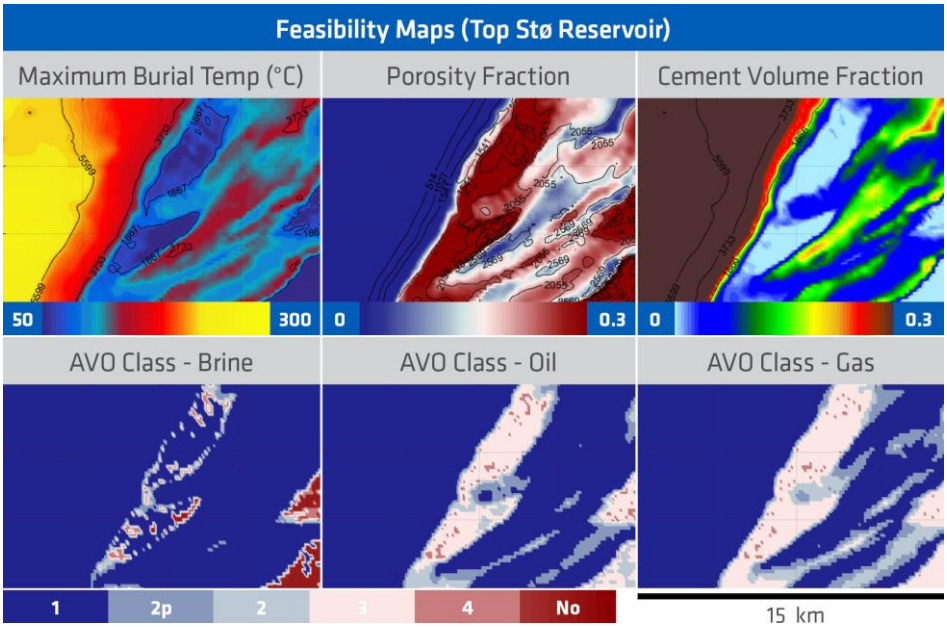

Figure 4. Rock property and AVO feasibility maps in an area focusing on Upper Jurassic fault blocks where Stø Fm is the target reservoir. Contours in upper left subplot are that of maximum burial, upper middle of uplift, and upper right of burial depth, all units being in metres. From Avseth et al. (2020b).

For the specific scenario parameters used in Figure 3, it was observed that while an uncertainty of 30% in the grain size does not lead to a very different outcome, a 30% uncertainty in the uplift will have a significant impact on potential reserves. An exploration team armed with such information might want to spend some extra time derisking this lead to reduce the uncertainty associated with the uplift. Note that many parameters will be tested in a real exercise because *every location is different*.

The Optimum Seismic Platform and Potential Pitfalls

My third and fourth webinars titled 'Low Frequencies: Where Are We Now?' and 'AVO Lessons From the Broadband Seismic Revolution', respectively, consider various issues relevant to the low-frequency amplitude and phase content of seismic data.

It is established that pre-stack simultaneous AVA inversion without a low-frequency elastic model of the earth that spans all frequencies below the lowest useful frequency signals in the seismic data is 'relative' only. Broadband seismic methods such as GeoStreamer have useful frequency content in the 2 to 4 Hz range, but we need a robust source of elastic information below 3 or 4 Hz for the inverted elastic parameters to be 'absolute' in the sense that they are quantitatively accurate. Where well control exists, co-kriging of the seismic velocity model and the well data has historically been used to interpolate elastic well properties to smooth geologic trends. However, the typically poor spatial sampling of well locations introduces structural uncertainties into the interpolated model—particularly above about 1 to 2 Hz, and the infamous 'low frequency gap' between this elastic model information and the low frequency end of the seismic data reduces confidence in the accuracy of any inverted elastic parameters.

However, the low frequency gap can be closed if we can build high-resolution velocity models augmented by reliable rock-physics transformations. FWI is the obvious solution to build high-resolution and geologically-consistent velocity models, but there are many technical issues to consider—and one of the most famous challenges is that of cycle-skipping—wherein the synthetic shot gather modeled with an (imperfect) FWI velocity model iteration is misaligned with the field data version by more than half a frequency cycle. This is the main reason why FWI practitioners historically sought to have very rich low frequencies in the field data—to help reduce the traditional dependence upon a very accurate starting model, and to help FWI updates converge without failing outright, or creating massive artifacts in the model. But does this therefore create a paradox? Without very-low frequency (VLF) amplitudes in the field data, will FWI fail to work in a stable manner, and without an accurate FWI model, how can we exploit rock physics transformations from velocity to low frequency elastic impedance models…?

Fortunately, not all is lost. It can be shown that modern multisensor broadband seismic data + a new suite of FWI solutions provides the stable platform necessary. Through a combination of a new wave equation formulation, a new extended time-warping misfit function (Huang et al., 2021), and a dynamically-weighted FWI gradient that removes unwanted high-wavenumber migration artifacts from the model, the cycle-skipping problems of the past can generally be avoided. A robust FWI solution that has greatly reduced assumptions about low frequency content in the field data can recover much deeper updates with conventional offset ranges, requires no density model or hard boundaries in the initial velocity model to exploit the reflection information in field gathers, and can yield models that are very high-resolution and entirely geologically consistent. But how can such FWI models augment rock physics—beyond reconstructing the burial history necessary to build better rock models?

Figure 5 is from offshore Canada, where FWI was used to augment absolute seismic inversion—despite negligible well control. PGS, in partnership with TGS, have acquired more than 20 000 square kilometres of multisensory GeoStreamer seismic data in Newfoundland and Labrador since 2011. There are only three wells in this regional set of surveys, each of which demonstrated the presence of regional source rocks. All three wells were used for a regional rock physics analysis that accounted for burial depth and the elastic properties corresponding to each lithology intersected by the wells—as described in the workflows above. It was established that the separation between the brine and oil-saturated response on Vp/Vs versus P-impedance crossplots is quite weak, but gas versus oil saturation is more distinct. Correspondingly, broadband GeoStreamer data that accurately captured AVO information was deemed to be critical.

In Figure 5 the FWI model information at the Great Barasway well location up to 6 Hz was used to build the low frequency model—using very robust rock physics transformations, and all higher frequency information was derived from the broadband GeoStreamer seismic data during the pre-stack simultaneous AVA inversion. The green curves on the right of Figure 5 correspond to the well log data filtered to the seismic frequencies, and the red curves correspond to the low frequency model derived from the FWI velocities. The inversion sequence estimated the elastic properties, as well as the scaling for the Vp/Vs trend to ensure the background model was accurate. A three-term Aki-Richards AVO equation was used with five angle stacks up to a maximum angle of 55 degrees. Several amplitude anomalies with fluid effects potentially representative of hydrocarbons were identified, merit further investigation, and demonstrate that despite the very sparse regional well control, the combination of a careful regional rock physics analysis and the availability of broadband GeoStreamer data and high-resolution FWI velocities meant that absolute elastic attributes could be inverted from the data. Results are shown in My third webinar titled 'Low Frequencies: Where Are We Now?'

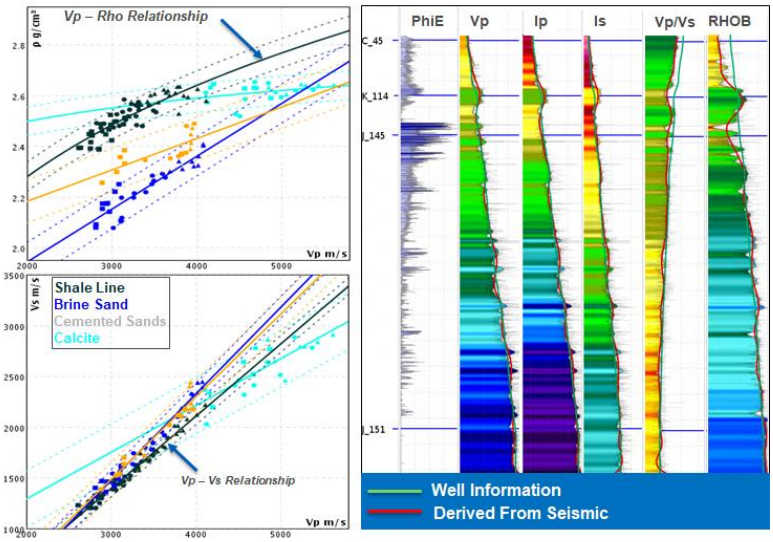

Figure 5. Elastic low-frequency model building using rock-physics transforms of FWI models.

My fourth webinar titled 'AVO Lessons From the Broadband Seismic Revolution' moves on from looking at low-frequency AVO issues in seismic data, and instead considers low-frequency phase issues. A decade of processing broadband marine seismic data illustrates that the wavefield separation of multisensor streamer data automatically accounts for frequency-dependent variations in the emergence angle of the recorded wavefirelds; including effects associated with variable sea surface height or variable streamer depths. If any broadband processing does not account for such effects, all kinds of amplitude and phase errors are introduced for a broad range of frequencies around the notch frequencies—and most serious at the lowest frequencies.

Also of relevance to low frequencies, a published study conducted a detailed elastic synthetic modeling and pre-stack simultaneous AVA inversion exercise to quantify the impact of various deliberate perturbations of far angle stacks—where experience says problems are more likely to occur. The observations confirmed that frequency-dependent phase rotations can be difficult to detect on post-stack data, may be more detectable on pre-stack data, and the phase shift problem is more nefarious at low frequencies. The pre-stack data most affected by (imperfect) broadband processing artifacts and low-frequency phase rotation is the far-angle data. I used two case studies in my fourth webinar to illustrate how such errors can translate to errors in the stability and fidelity of the Gradient terms computed during AVA studies. Errors in the gradient term will correspondingly translate to noisy and erroneous S-impedance and Vp/Vs ratio being derived during simultaneous pre-stack AVA inversion. The collective lesson is to pursue broadband preconditioning solutions that are as deterministic and predictable as often as possible, and less likely to introduce statistical variability into elastic attributes.

Validation of New Acquisition and Imaging Platforms

We have a very flexible portfolio of acquisition, model building and imaging solutions at PGS—but how do we know the elastic attributes we derive from the various pre-stack data are valid—or that the predicted lithology and fluid properties are accurate? My fifth webinar titled 'Global Rock Physics Lessons and Success Stories' uses three case studies to illustrate that with the benefit of appropriate rock physics workflows, fundamentally different acquisition, or fundamentally different imaging platforms can be used with confidence in QI projects.

A new acquisition methodology known as GeoStreamer X combines several technology innovations to optimize seismic image quality and resolution from the seafloor to the deepest targets. In a survey located in the South Viking Graben, two new azimuths of data were acquired over an existing azimuth of GeoStreamer data. The new azimuths used triple-source shooting with wide source separation to benefit the near-offset coverage for shallow imaging, two long streamer tails to benefit deep FWI velocity model updates, and dense GeoStreamer separation with deep tow to optimize resolution and data quality at all depths. As expected, the new seismic images show substantially better event resolution and character at all depths. A well-to-seismic tie estimation showed that the cross-correlation between the seismic data and the well data from more than 10 wells exceeded 80%, and an excellent broadband wavelet could be extracted from the data.

All three contributing surveys were binned and regularized into six unique azimuths, and these data for four angle stacks were used to compute the Intercept and both the isotropic and anisotropic Gradient terms. The Vp/Vs ratio from the isotropic Gradient estimation shown in Figure 6 is an example of data that is rich in subsurface information being used quantitatively with great effect. This image around the Lille Prinsen oil discovery suggests an untested hydrocarbon accumulation that is possibly oil, to the right of the main horst feature. Overall, various quantitative analyses guided by rock physics processes demonstrate that the GeoStreamer X acquisition platform is clearly beneficial for more quantitatively accurate and reliable interpretation.

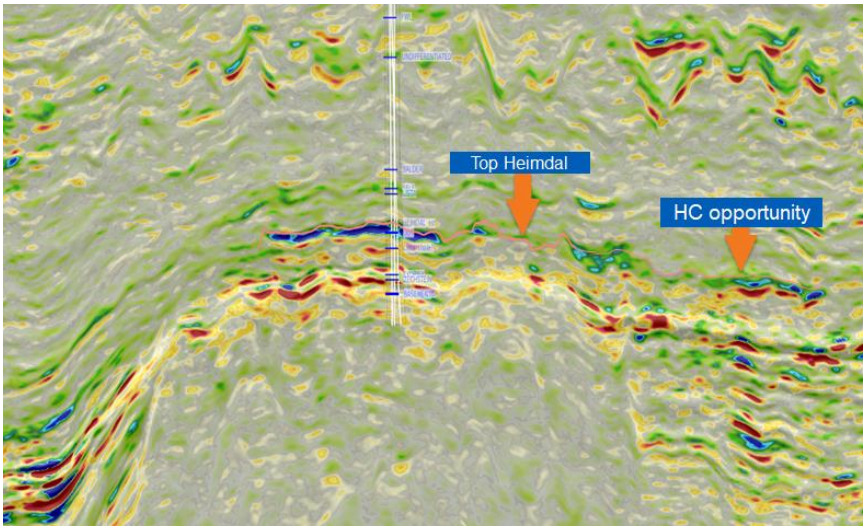

Figure 6. Vp/Vs image inverted from GeoStreamer X data using an Intercept and isotropic Gradient estimation from six azimuths and three angle stacks for each azimuth of data.The well intersection corresponds to the Lille Prinsen oil discovery. The right-hand arrow indicated a potentially untested oil accumulation.

The webinar titled 'Global Rock Physics Lessons and Success Stories' also illustrates a solution to very-shallow reservoir imaging and characterization challenges when the near-angle information for characterizing very shallow targets is missing from legacy multisensor data. This type of challenge is not only relevant to shallow conventional hydrocarbon reservoirs—it is also relevant to scenarios such as carbon capture and storage (CCS) where a precise knowledge of shallow aquifer seal integrity is critical.

Acknowledgments

I particularly thank Per Avseth, Cyrille Reiser and Nizar Chemingui for their gracious contribution of time and resources over many years.

Suggested Reading Material

- Huang, G., Ramos-Martínez, J., Yang, Y., and Chemingui, N., 2021, FWI in extended domain using time-warping: 91st Annual Technical Program, SEG, Expanded Abstracts, in press.
- Reiser, C., 2021, Make better decisions with multi-azimuth multisensor quantitative interpretation | A case study from the South Viking Graben: PGS webinar. https://www.pgs.com/media-and-events/webinar-library/europe-africa--middle-east/
- Ruiz, R., 2021, rockAvo | Experience Realtime Exploration Analysis and Rock Property Perturbation: PGS webinar. https://www.pgs.com/media-and-events/webinar-library/technology-webinars/webinars/rockavo--experience-realtime-exploration-analysis-and-rock-property-perturbation/